

Performance of genomic data sets on the estimation of the divergence time of New World and Old World anthropoids

C.G. Schrago and C.M. Voloch

Departamento de Genética, Universidade Federal do Rio de Janeiro, Brasil

Corresponding author: C.G. Schrago
E-mail: carlo.schrago@gmail.com

Genet. Mol. Res. 13 (1): 1425-1437 (2014)
Received December 4, 2012
Accepted September 3, 2013
Published March 6, 2014
DOI <http://dx.doi.org/10.4238/2014.March.6.1>

ABSTRACT. The origin of New World anthropoids has received renewed attention since the advent of molecular dating methods that relax the assumption of a strict molecular clock. However, the studies conducted to date have estimated the time of the separation of New World and Old World anthropoids at values as different as 70 and 22 Ma. With the aim of investigating the source of the discrepancies in the inferred ages, we have compared the performance of mitochondrial and nuclear markers in two pairs of datasets. We show that in the larger genomic samples, the dates of the separation of New and Old World anthropoids estimated from nuclear and mitochondrial data are significantly different. The precision of the estimates demonstrated that both markers rendered significantly different estimates. However, parametric estimates from the large nuclear dataset were highly cross-correlated. Cross-correlation of absolute divergence times and evolutionary rates was as great as -96%. Consequently, the age estimates from the large nuclear data were not reproducible, because Markov chains were unable to reach the same parametric values independently, even with the adoption of additional information from calibration priors. Thus, because branch length decomposition was not achieved, a comparison of the genomic

age estimates from nuclear and mitochondrial datasets was statistically impractical. We demonstrate the importance of examining the output of Markov chain Monte Carlo analyses for correlation between rate and time in studies that use phylogenomic datasets to examine the chronological scales of primate evolution.

Key words: Eocene; Oligocene; Biogeography; South America; Bayesian relaxed clock

INTRODUCTION

One of the long-standing issues in primatology is the evolutionary circumstances surrounding the origin of the New World anthropoids (NWA) (Fleagle, 1998). This issue is fundamentally associated with the conspicuous geographical distribution of anthropoid species. In the New World, all endemic primate fauna are anthropoids of the Parvorder Platyrrhini (Wilson and Reeder, 2005), a monophyletic group from which the first fossil found, *Branisella boliviana*, dates back to the Oligocene, ca. 27 Ma (Takai and Anaya, 1996). Because the fossil record of early anthropoids is older than the age of *Branisella* (Williams et al., 2010), the origin of NWA should not be a biogeographical problem, except that the early fossils of anthropoids were found in Africa and Asia, while early platyrrhines were found exclusively in South America, and were formed when that continent was an isolated landmass. Therefore, the circumstances that allowed the ancestors of the NWA to reach South America, an isolated island-continent, during the Eocene and Oligocene, remain unclear (Hoffstetter, 1974; de Oliveira et al., 2008).

In an attempt to clarify this issue, several authors have applied molecular dating techniques to estimate the timing of the genetic separation of New and Old World anthropoids (OWA, Parvorder Catarrhini) (Schrago and Russo, 2003; Opazo et al., 2006; Poux et al., 2006; Schrago, 2007). The rationale of these studies is that, because the NWA are monophyletic, the age of the NWA/OWA genetic separation might be a good indicator of the time at which the ancestral Platyrrhini stock arrived in South America. However, estimates of the time of the Platyrrhini/Catarrhini split vary greatly among studies (Glazko and Nei, 2003; Yang and Yoder, 2003; Kullberg et al., 2006; Steiper and Young, 2006; Babb et al., 2010), placing the age of the separation as early as the late Cretaceous, ca. 70 Ma (Arnason et al., 2000), or as late as the early Miocene, 22.6 Ma (Poux and Douzery, 2004). Even with the exclusion of outliers, this interval is too large to permit any meaningful evaluation of the biogeographic scenarios of NWA origins.

Evidently, this discrepancy may be caused by several factors, such as the molecular dating method applied (classical clock vs. Bayesian relaxed methods), the calibration information used (internal vs. external calibrations, punctual vs. probabilistic calibrations), and the number and choice of genes used in the analysis. The number of possible combinations of the above criteria is large and, to complicate matters further, the reasons for the differences between estimates may be multifactorial. Thus, approaches such as those implemented by Hedges et al. (2006), who used the mean value of several estimates for a given divergence, are justified. The rough average of several chronological estimates, however, cannot be used to determine which factor(s) is responsible for the observed parametric variance.

In this sense, it is interesting to note that the oldest estimates for the Platyrrhini/Catarrhini separation were obtained using mitochondrial genes (Arnason et al., 2000; Arnason and Janke, 2002; Yang and Yoder, 2003; Yoder and Yang, 2004), while younger estimates were inferred from nuclear data (Nei and Glazko, 2002; Poux and Douzery, 2004). This motivated us to investigate whether the source of the molecular marker (mitochondrial or nuclear) would influence the estimate of the age of the New World and Old World primate divergence. Our hypothesis is that when genomic datasets are investigated, estimates may converge to the same parametric value because of the larger sample sizes. In fact, when genomic datasets are considered under the same set of calibration information and methods, a significant difference is found, and nuclear genes date the NWA/OWA split at younger ages than mitochondrial genes. These results indicate that large data sets of nuclear and mitochondrial genes produce statistically significant different estimates for the date of this split. However, because of the large time-rate cross-correlation, the estimates obtained from the large nuclear data set were not reproducible, even if additional calibration information is provided. Therefore, this difference between nuclear and mitochondrial data is explained by the failure of the relaxed molecular clock to decompose branch lengths in absolute rates and times when the length of the sequences studied is very large (>1 million nucleotide sites). Thus, we recommend that the efficacy of the time-rate decomposition should be verified when reporting timescales calculated using phylogenomic datasets.

MATERIAL AND METHODS

Datasets and alignment

Two nuclear datasets and two mitochondrial datasets with varying taxonomic sampling were assembled for this study. The first pair of datasets, henceforth referred to as the *small* datasets, consist of a nuclear dataset and a mitochondrial dataset with the same taxonomic composition of 34 terminals each, and containing, as far as possible, the same species. When sequence information was not available for both markers in one species, we sampled another phylogenetically close species. For instance, *Microcebus* was sampled in the nuclear dataset and *Lemur* was used in the mitochondrial analysis; both are Lemuriformes primates. Similarly, *Otolemur* (nuclear) was paired with *Galago* (mitochondrial), another Loriformes. The Sciuridae are represented by the genus *Spermophilus* in the nuclear dataset and *Sciurus* in the mitochondrial dataset. Finally, *Dipodomys* and *Jaculus* represent the Sciurognathi in the nuclear and mitochondrial datasets, respectively (Figure 1a and b). The small mitochondrial dataset consists of 13 protein-coding genes, concatenated to yield an 11,763-bp supermatrix. The small nuclear dataset consists of 15 protein coding genes selected from the OrthoMam database (Ranwez et al., 2007). The 15 genes were selected with the goal of obtaining a dataset of nuclear markers with heterogeneous evolutionary rates. The small nuclear alignment consists of 50,928 nucleotides (Table 1).

The second pair of datasets, henceforth referred to as the *large* datasets, was assembled to achieve the maximum amount of data for divergence time inference. In the nuclear dataset, we selected all orthologous genes available for the primates in the OrthoMam database for which the molecular clock hypothesis was not rejected by the likelihood ratio test (LRT; Felsenstein, 1988). This consists of 1102 out of 5730 genes. LRT was performed with the

baseml program in the PAML 4.4 package (Yang, 2007). *Bos* was used as an outgroup because its inclusion increased the number of orthologous genes that failed to reject the strict clock hypothesis. Therefore, we expect this to be an ideal assembly of genes for divergence time inference. The final supermatrix composed of “clock-like” genes is 1,075,872-bp long (Figure 2a). The nuclear genes used in the large dataset are listed in the supplementary material (Table 1SM). Because the number of mitochondrial coding genes (13) could not be increased, we sampled mitochondrial genomes from all mammalian genera available in NCBI, for 179 sequences (Figure 2b). The accession numbers for the mitochondrial genomes of the species used in the analysis are available at www.ncbi.nlm.nih.gov/sites/genome.

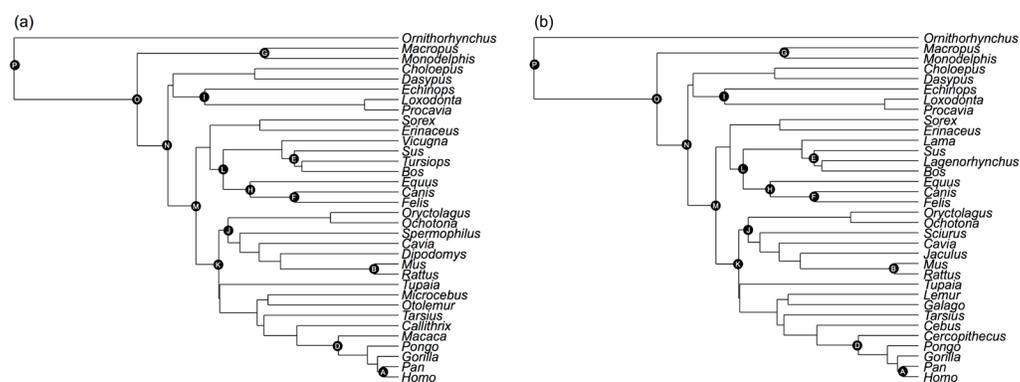


Figure 1. Tree topologies of the pair of small datasets used in this study. **A.** Nuclear dataset, **B.** mitochondrial dataset.

Table 1. Orthologous groups from OrthoMam used in the analysis.

| EnsEMBL code | Gene name (OrthoMam) | Length (bp) | Relative rate* |
|-----------------|----------------------|-------------|----------------|
| ENSG00000160551 | TAOK1 | 3,405 | 0.35 |
| ENSG00000070961 | ATP2B1 | 3,846 | 0.41 |
| ENSG00000163939 | PBRM1 | 5,157 | 0.43 |
| ENSG00000198408 | MGEA5 | 2,997 | 0.43 |
| ENSG00000144290 | SLC4A10 | 5,067 | 0.5 |
| ENSG00000157680 | DGKI | 3,090 | 0.64 |
| ENSG00000071794 | HLTF | 3,075 | 0.65 |
| ENSG00000115839 | RAB3GAP1 | 3,039 | 0.77 |
| ENSG00000102385 | DRP2 | 3,051 | 0.89 |
| ENSG00000166387 | PPFIBP2 | 3,054 | 0.93 |
| ENSG00000127463 | KIAA0090 | 3,024 | 1.06 |
| ENSG00000143924 | EML4 | 3,039 | 1.19 |
| ENSG00000122025 | FLT3 | 3,036 | 1.27 |
| ENSG00000075856 | SART3 | 3,033 | 1.3 |
| ENSG00000157404 | KIT | 3,015 | 1.38 |

(*) Relative evolutionary rate was calculated according to the procedure of Criscuolo et al. (2006).

Divergence time analysis

Divergence time analyses were conducted in BEAST 1.6.2 (Drummond and Rambaut, 2007) under the Bayesian paradigm, using the uncorrelated lognormal model as the evolutionary

rate prior (Drummond et al., 2006). The GTR+G+I model of nucleotide substitution was used in every analysis. Posterior distributions of parameters were obtained via the Markov chain Monte Carlo (MCMC) method. In every analysis, Markov chains were run for 30,000,000 generations and sampled every 1000th cycle, yielding 30,000 samples from which 10% was discarded as burn-in.

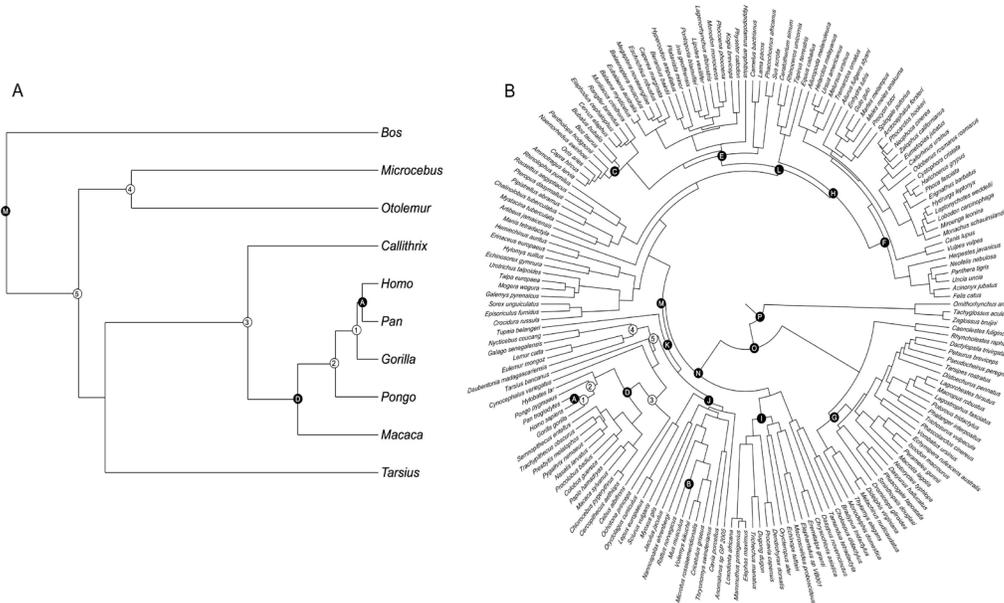


Figure 2. Tree topologies of the pair of large datasets used in this study. **A.** Nuclear dataset, **B.** mitochondrial dataset.

MCMC output analysis

Chain convergence was monitored by calculating the effective sample size (ESS), which was >500 in all samples, and by implementing the Heidelberger and Welch test (1983) in the CODA package (Plummer et al., 2006) of the R programming environment (www.r-project.org). Relaxed molecular clock methods, as implemented in BEAST, aim to decompose branch lengths and independently estimate absolute substitution rates and divergence times. Thus, to check for a strong correlation between divergence times and mean substitution rates (the meanRate parameter of BEAST) that would indicate that decomposition was not efficiently achieved, we estimated the cross-correlation between rates and times also using the CODA package. As a means of comparing the behavior of the estimates for the Platyrrhini/Catarrhini divergence with another primate split, we also studied the date of the separation of humans and chimps. The *Homo/Pan* divergence is a standard calibration node within primates, having occurred between 10 and 6.5 Ma (Benton and Donoghue, 2007). The significance of the difference between the posterior distributions of the divergence time estimates was evaluated using the approach described in Loss-Oliveira et al. (2012). The rationale for this approach is that, in a Bayesian framework, if two posterior distributions are statistically equivalent, the distribution of the difference, *D*, between the pair of parametric values from each distribution collected during MCMC should include zero within the 95% highest probability density (HPD) interval.

Calibration information

Two calibration schemes were adopted in this study. In the first scheme, the calibration data chosen were based exclusively on the fossil record, following Benton and Donoghue (2007), and were applied to the nodes highlighted in Figures 1 and 2. All calibrations were modeled by normal distributions in which the mean was set at the average between the minimum and maximum values suggested by Benton and Donoghue (2007); the standard deviation was set such that the 95% highest probability density (HPD) interval of the distribution was delimited by these minimum and maximum values (Table 2). It is important to note that in the first pair, exactly the same calibration information was applied in the nuclear and mitochondrial datasets, whereas in the larger dataset (which maximized the information for divergence time estimation), although the calibration and taxonomic compositions were different, we expected that the parameters would be estimated with reduced variance as a consequence of increased sample size (Casella and Berger, 2002).

Table 2. Calibration information used as divergence time priors.

| Node* | Divergence | Normal prior mean | Normal prior SD |
|-------|---|-------------------|-----------------|
| A | <i>Homo/Pan</i> | 8.3 | 0.9 |
| B | <i>Mus/Rattus</i> | 11.7 | 0.4 |
| C | Bovinae/Antilopinae | 23.4 | 2.6 |
| D | Hominoidea/Cercopithecoidea | 28.5 | 2.8 |
| E | Ruminantia/Tylopoda-Suiformes | 50.9 | 1.3 |
| F | Caniformia/Feliformia | 53.3 | 2.6 |
| G | Ameridelphia/Australidelphia | 66.4 | 2.5 |
| H | Carnivora/Perissodactyla | 66.8 | 2.2 |
| I | Afrosoricida/Tubulidentata-Paenungulata | 80.7 | 16.5 |
| J | Glires | 81.0 | 10.0 |
| K | Archonta/Glires | 81.0 | 10.0 |
| L | Ferungulata | 104.2 | 4.5 |
| M | Euarchontoglires/Laurasiatheria | 104.2 | 4.5 |
| N | Boreoeutheria/Xenarthra | 104.2 | 4.5 |
| O | Eutheria/Metatheria | 131.5 | 3.5 |
| P | Therimorpha/Australosphenida | 176.8 | 7.3 |

(*) As displayed in Figures 1 and 2.

A second calibration scheme was applied exclusively to the large datasets in order to investigate whether the difference found between nuclear and mitochondrial estimates was robust to the calibrations used. We adopted five additional prior calibrations for primate divergences that were mostly borrowed from dos Reis et al. (2012). The new calibrations used were the split between the *Gorilla* and *Homo/Pan*, the *Pongo* divergence, the Lemuriformes/Loriformes separation, the Strepsirrhini/Haplorrhini split and, finally, the Platyrrhini/Catarrhini divergence (Table 3). In this second calibration scheme, divergence time analyses were run 10 times independently. Therefore, we have also measured the extent of the convergence of the MCMC runs.

RESULTS

Under the first calibration scheme, analyses of the pair of small datasets (with identical calibration and taxonomic compositions) resulted in posterior distributions that dated the age of the Platyrrhini/Catarrhini divergence at 38.6 Ma using nuclear genes (95% HPD

interval: 26.9-50.7 Ma) and at 50.1 Ma using mitochondrial genes (95% HPD interval: 36.8-64.9 Ma) (Table 4). The standard deviations of the posterior distributions of divergence times were large (6.6 Ma for the nuclear and 7.4 Ma for the mitochondrial datasets), resulting in an overlap of 13.9 Ma between 95% HPD intervals (Figure 3a). The posterior distributions of the age of the split using the small sets of nuclear and mitochondrial genes were statistically equivalent. The 95% HPD interval of the distribution of the difference between the samples collected during MCMC included zero, varying from -7.4 Ma to 29.3 Ma.

Table 3. Additional primate calibration information used as divergence time priors.

| Node ¹ | Divergence | Calibration prior |
|-------------------|---------------------------|----------------------------|
| 1 | <i>Gorilla</i> /Hominini | U (7.5, 34.0) ² |
| 2 | <i>Pongo</i> /Homininae | U (11.2, 34.0) |
| 3 | Platyrrhini/Catarrhini | N (40.0, 10.0) |
| 4 | Lemuriformes/Loriiformes | U (33.7, 55.6) |
| 5 | Strepsirrhini/Haplorrhini | U (55.6, 104.2) |

¹As displayed in Figure 2. ²U (min, max), N (mean, SD).

Table 4. Divergence time estimates of the Platyrrhini/Catarrhini separation and the human/chimp split.

| | Datasets | | | | | |
|-----------------|---------------|---------------|--|---------------------|---------------------|---------------------------------|
| | Small nuclear | Large nuclear | Additional priors nuclear ¹ | Small mitochondrial | Large mitochondrial | Additional priors mitochondrial |
| NWA/OWA | 38.6 ± 6.6 | 38.6 ± 1.6 | 43.1 ± 10.3 | 50.1 ± 7.4 | 53.1 ± 3.4 | 48.8 ± 0.6 |
| <i>Homo/Pan</i> | 7.9 ± 0.9 | 6.9 ± 0.3 | 8.1 ± 1.8 | 8.1 ± 0.9 | 8.1 ± 0.9 | 7.6 ± 0.1 |

(¹) Average values and standard deviations across the 10 independent runs.

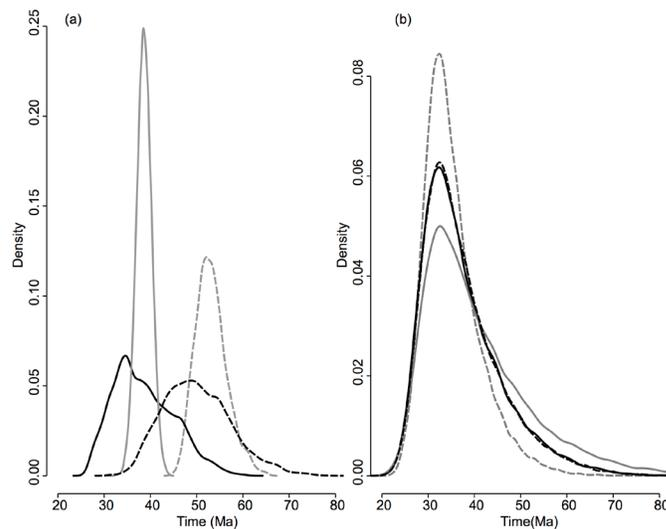


Figure 3. A. Posterior distributions of the age of the Platyrrhini/Catarrhini divergence. **B.** Prior distributions of the age of the Platyrrhini/Catarrhini divergence. Small nuclear (solid black line), small mitochondrial (dashed black line), large nuclear (solid grey line) and large mitochondrial (dashed grey line) datasets.

In the large datasets, the NWA/OWA separation was estimated to have taken place at 38.6 Ma (95% HPD interval: 36.0-41.8 Ma) by the nuclear data and at 53.1 Ma (95% HPD interval: 47.0-60.3 Ma) by the mitochondrial data (Figure 3a). The standard deviations of the posterior distributions were considerably reduced (1.6 Ma for nuclear and 3.4 Ma for mitochondrial genes); consequently, there was no overlap between the 95% HPD intervals.

All divergence time estimates were different from their priors in the first calibration scheme. The prior distributions of the Platyrrhini/Catarrhini divergence times were similar among the datasets studied (Figure 3b), with means varying from 35.2 Ma (mitochondrial, large sample size) to 40.3 Ma (nuclear, large sample size). The standard deviation of the prior distributions also varied little, from 6.1 Ma (mitochondrial, large sample size) to 11.3 (nuclear, large sample size).

The age of the *Homo/Pan* divergence was dated at 7.9 ± 0.9 Ma and 8.1 ± 0.9 Ma by the small datasets composed of nuclear and mitochondrial genes, respectively. When large genomic datasets were used, the split was inferred at 6.9 ± 0.3 Ma for the nuclear and 8.1 ± 0.9 Ma for the mitochondrial dataset. Thus, the large nuclear dataset also dated the age of the human/chimp separation at a younger value.

The cross-correlation between the age of the Platyrrhini/Catarrhini split and the mean substitution rate was estimated to be -0.05 in the nuclear dataset and -0.41 in the small mitochondrial dataset (Table 5). The analysis of large datasets resulted in rate-time cross-correlations of -0.31 (mitochondrial) and -0.96 (nuclear). The *Homo/Pan* divergence followed the same trend: the cross-correlation between rate and time was inferred at -0.05 for the small nuclear set and -0.06 for both the small and large mitochondrial datasets. The rate-time cross-correlation was also high in the large nuclear dataset (-0.89).

Table 5. Cross-correlations between mean evolutionary rate and divergence times.

| | Datasets | | | | | |
|-----------------|---------------|---------------|--|---------------------|---------------------|---------------------------------|
| | Small nuclear | Large nuclear | Additional priors nuclear ¹ | Small mitochondrial | Large mitochondrial | Additional priors mitochondrial |
| NWA/OWA | -0.05 | -0.96 | -0.82 ± 0.2 | -0.41 | -0.31 | -0.10 ± 0.1 |
| <i>Homo/Pan</i> | -0.05 | -0.89 | -0.67 ± 0.3 | -0.06 | -0.06 | -0.02 ± 0.1 |

(¹) Average values and standard deviations across the 10 independent runs.

When additional calibration priors were used in the large data set (the second calibration scheme), the average age of the basal anthropoid node across the 10 independent runs was 48.8 ± 0.6 Ma in the mitochondrial data set (Figure 4), while the average age of the human/chimp divergence across the replicates was 7.6 ± 0.1 Ma (Table 4). In the nuclear data set, the average age of the Platyrrhini/Catarrhini split across the independent runs was 43.1 ± 10.3 Ma. For the *Homo/Pan* divergence, the average was 8.1 ± 1.8 Ma. The average cross-correlations between times and rates among replicates in the mitochondrial data set was -0.10 ± 0.1 (NWP divergence) and -0.02 ± 0.1 (*Homo/Pan* split). In the nuclear data, the average values were -0.82 ± 0.2 and -0.67 ± 0.3 for the basal anthropoid and human/chimp separations respectively (Table 5).

Therefore, the additional calibration priors reduced, on average, the difference between the ages of the Platyrrhini/Catarrhini separation from the large mitochondrial and nuclear data sets. Figure 4 illustrates that, while mitochondrial runs converged to the same posterior distribution, the independent runs of the large nuclear data set have not reached the same posterior density. Actually, the nuclear runs yielded the oldest and the youngest estimates of the NWA/OWA split. Thus, MCMC runs of the large nuclear alignment have not converged.

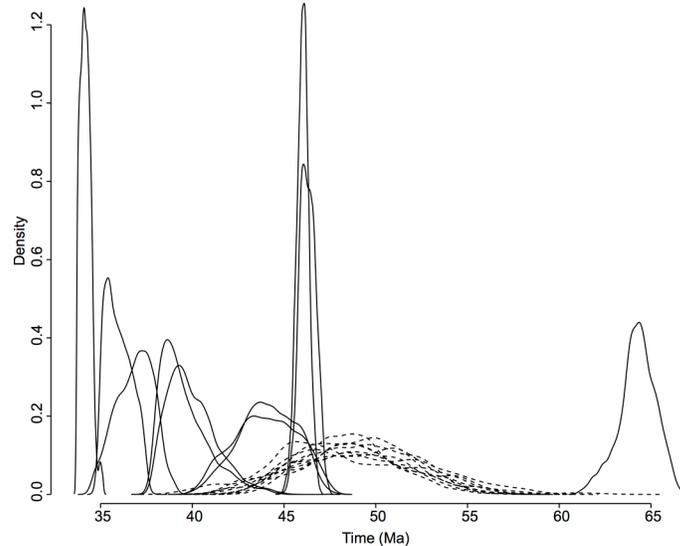


Figure 4. Posterior densities of the 10 independent runs under the second calibration scheme. Solid and dashed lines represent the large nuclear and mitochondrial data sets respectively.

DISCUSSION

The Bayesian estimates of the age of the genetic separation of NWA and OWA inferred from nuclear and mitochondrial data were significantly different when using large phylogenomic sample sizes that increased the alignment length or taxonomic sampling under the first scheme of calibration information. Mitochondrial and nuclear estimates consistently shifted to different age values with reduced variance (Figure 3a). As the prior distribution of the date of the Platyrrhini/Catarrhini separation inferred from the mitochondrial dataset was indistinguishable from that of the nuclear dataset (Figure 3b), the shift of the posterior distributions could only be driven by the likelihood of the data.

However, under the first calibration scheme, the inferred age of the *Homo/Pan* separation was also younger in the large nuclear dataset. The concomitant shifts in the estimates of the human/chimp and Platyrrhini/Catarrhini divergences in the large nuclear analysis demonstrated that, in this dataset, time parameters were correlated because evolutionary rates and times were not independently estimated. The strong cross-correlation is readily observed in plots of the joint marginal posterior distributions of the mean substitution rates and the ages of the Platyrrhini/Catarrhini and *Homo/Pan* splits (Figure 5).

If times and rates were not effectively decomposed, we expect that independent runs of the analysis will be unable to reach a stable value. This is exactly what was found in the analysis of the nuclear data set with additional calibration priors (Figure 4). Therefore, our results showed that, even using additional calibration priors, the ineffective decomposition of the evolutionary distance in absolute times and rates severely affected divergence time estimation using the large nuclear alignment.

It is worth mentioning that cross-correlation between time and rate parameters is gen-

erally reduced by the adoption of informative calibration priors (Rannala and Yang, 2003). Here, the use of additional calibration information did reduce the difference between the large mitochondrial and large nuclear data sets, indicating that the gap between mitochondrial and nuclear estimates observed in the large nuclear analysis under the first calibration scheme was likely an artifact. Nevertheless, in contrast with the large mitochondrial data set, the 10 independent MCMC runs of the large nuclear data set were unable to reach a stable value for the NWA/OWA separation.

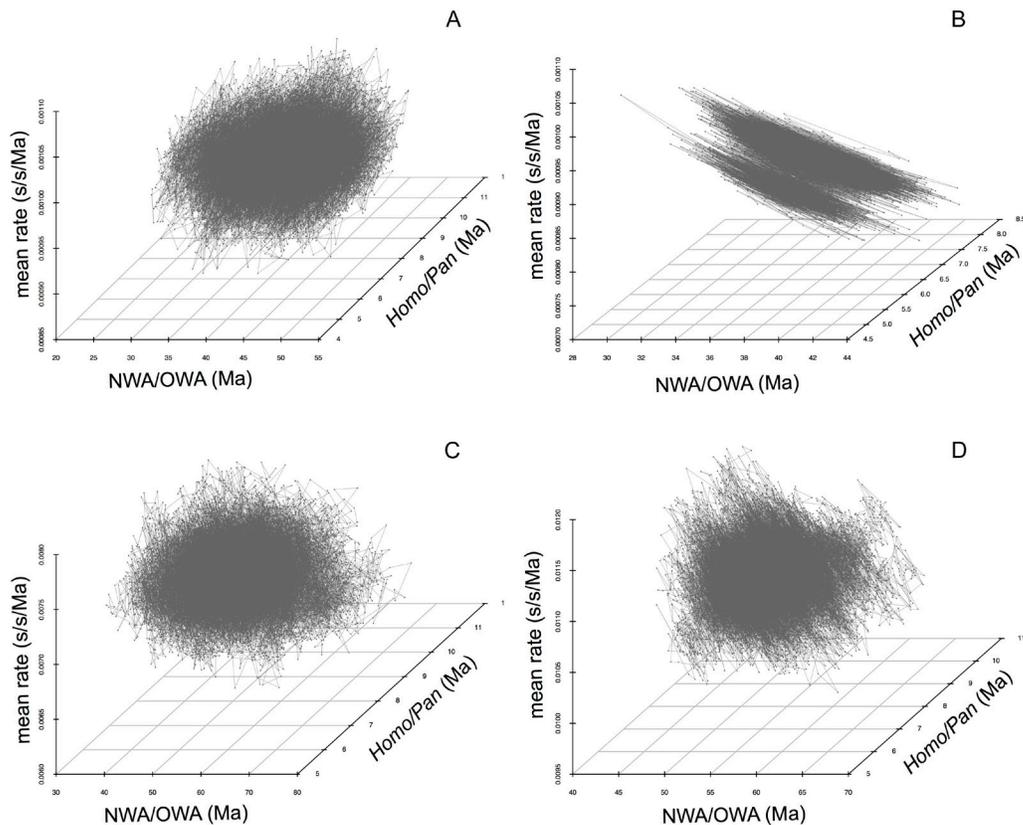


Figure 5. Parametric values collected during the MCMC run for the mean absolute evolutionary rate (in substitutions/site/Ma), the age of the *Homo/Pan* divergence and the age of the NWA/OWA separation under the first calibration scheme. Points were plotted in three-dimensional space to represent the joint posterior distribution of the estimates. Lines connecting points were drawn to show the complete MCMC walk-through parametric space. Notice the strong cross-correlation in B., the large nuclear dataset. **A.** Small nuclear dataset, **B.** large nuclear dataset, **C.** small mitochondrial dataset, and **D.** large mitochondrial dataset.

Independent of the calibration scheme adopted, the large nuclear data set resulted in high values of time-rate cross-correlations. Thus, both schemes of calibration priors were unable to inform the posterior distribution of parameters. Bayesian inference is roughly the product of the data likelihood and the prior distribution. Calibration information is entered as

prior distribution of the absolute age of the nodes (Thorne et al., 1998; Thorne and Kishino, 2002). Data likelihood is calculated using Felsenstein's (1981) algorithm, which uses branch lengths as parameters and not absolute rates and times independently (Yang, 2006). When the sample size is large, the error associated with the likelihood estimate is small. Consequently, the data likelihood predominates the posterior distribution of the parameter when the variance of the prior is large (Gilks et al., 1995). The small error associated with the maximum likelihood estimation is illustrated in Figures 3 and 4, in which the posterior density is narrowly distributed around the means in the large nuclear data set.

As the number of studies using large datasets to estimate primate divergence times is increasing (Steiper and Young, 2006; Chatterjee et al., 2009; Perelman et al., 2011), the issue reported in this study should be considered carefully. When alignments are large, we recommend that rate-time cross-correlations should be calculated, and that the analysis should be run as many independent times as possible. The usual measures of MCMC convergence, such as effective sample size and chain autocorrelation, are insufficient to verify the quality of chronological estimates in relaxed clock analysis. For instance, under the first calibration scheme, the effective sample sizes for the ages of the Platyrrhini/Catarrhini and *Homo/Pan* splits in the large nuclear dataset were 787.5 and 1085.1, respectively. Additionally, the autocorrelations of the Markov chains were very small for both parameters (0.05 and 0.06, respectively).

The impossibility of independent estimation of times and rates in the large nuclear data sets makes the age estimates obtained from the small datasets mostly suited for comparative purposes. Moreover, these datasets rendered posterior distributions that were statistically identical. Therefore, we may affirm that the Platyrrhini/Catarrhini split may have occurred as recently as 26.9 Ma or as long ago as 64.9 Ma. The range encompasses the minimum value of the 95% HPD interval from the posterior distribution of the small nuclear set, and the maximum value of the 95% HPD interval of the posterior from the small mitochondrial set, with mean age estimated at 44.3 Ma, which is very close to estimates from recent multi-locus studies. For instance, Steiper and Young (2009), Chatterjee et al. (2009), and Perelman et al. (2011) dated the split at 44.2 Ma, 43 Ma and 43.5 Ma, respectively. Note, also, that the use of additional calibration priors estimated the age of the NWA/OWA separation, on average, at the middle to late Eocene epoch, corroborating the recent dating analyses.

In conclusion, we have demonstrated that using the same calibration information, nuclear and mitochondrial markers yield different estimates of the Platyrrhini/Catarrhini separation. However, this difference should be interpreted statistically. When small datasets were used, this difference was not significant. When larger genomic datasets were used, however, the estimates from nuclear genes consistently placed the NWA/OWA split significantly later than did mitochondrial estimates. However, the strong cross-correlation between absolute divergence times and the mean evolutionary rate suggests that the relaxed molecular clock was incapable of decomposing branch lengths in absolute evolutionary rates and divergence times. The inability to perform independent estimations of times and rates also persisted when the large nuclear data set was analyzed adopting additional calibration information. Although the average difference between the nuclear and mitochondrial data sets was reduced, the independent runs of the large nuclear data set did not reach stable parametric values.

ACKNOWLEDGMENTS

This study was funded by the Conselho Nacional de Desenvolvimento Científico e

Tecnológico (CNPq) #308147/2009-0 and FAPERJ #E-26/103.136/2008, #110.838/2010, #110.028/2011, and #111.831/2011 to CG Schrago.

REFERENCES

- Arnason U and Janke A (2002). Mitogenomic analyses of eutherian relationships. *Cytogenet. Genome Res.* 96: 20-32.
- Arnason U, Gullberg A, Burguete AS and Janke A (2000). Molecular estimates of primate divergences and new hypotheses for primate dispersal and the origin of modern humans. *Hereditas* 133: 217-228.
- Babb PL, Fernandez-Duque E and Schurr TG (2010). AVPR1A sequence variation in monogamous owl monkeys (*Aotus azarai*) and its implications for the evolution of platyrrhine social behavior. *J. Mol. Evol.* 71: 279-297.
- Benton MJ and Donoghue PC (2007). Paleontological evidence to date the tree of life. *Mol. Biol. Evol.* 24: 26-53.
- Casella G and Berger RL (2002). *Statistical Inference*. 2nd edn. Brooks/Cole.
- Chatterjee HJ, Ho SY, Barnes I and Groves C (2009). Estimating the phylogeny and divergence times of primates using a supermatrix approach. *BMC Evol. Biol.* 9: 259.
- Criscuolo A, Berry V, Douzery EJP and Gascuel O (2006). SDM: A fast distance-based approach for (super) tree building in phylogenomics. *Syst. Biol.* 55: 740-755.
- de Oliveira FB, Molina EC and Marroig G (2008). Paleogeography of the South Atlantic: A Route for Primates and Rodents into the New World? In: *South American Primates, Developments in Primatology: Progress and Prospects*, Springer (Garber PA, Estrada A, eds.).
- dos Reis M, Inoue J, Hasegawa M, Asher RJ, et al. (2012). Phylogenomic datasets provide both precision and accuracy in estimating the timescale of placental mammal phylogeny. *Proc. Biol. Sci.* 279: 3491-3500.
- Drummond AJ and Rambaut A (2007). BEAST: Bayesian evolutionary analysis by sampling trees. *BMC Evol. Biol.* 7: 214.
- Drummond AJ, Ho SY, Phillips MJ and Rambaut A (2006). Relaxed phylogenetics and dating with confidence. *PLoS Biol.* 4: e88.
- Felsenstein J (1981). Evolutionary trees from DNA sequences: a maximum likelihood approach. *J. Mol. Evol.* 17: 368-376.
- Felsenstein J (1988). Phylogenies from molecular sequences: inference and reliability. *Annu. Rev. Genet.* 22: 521-565.
- Fleagle JG (1998). *Primate Adaptation and Evolution*. 2nd edn. Academic Press.
- Gilks WR, Richardson S and Spiegelhalter D (1995). *Markov Chain Monte Carlo in Practice*. 1st edn. Chapman and Hall/CRC.
- Glazko GV and Nei M (2003). Estimation of divergence times for major lineages of primate species. *Mol. Biol. Evol.* 20: 424-434.
- Hedges SB, Dudley J and Kumar S (2006). TimeTree: a public knowledge-base of divergence times among organisms. *Bioinformatics* 22: 2971-2972.
- Heidelberger P and Welch PD (1983). Simulation run length control in the presence of an initial transient. *Opns. Res.* 31: 1109-1144.
- Hoffstetter R (1974). Phylogeny and geographical deployment of primates. *J. Hum. Evol.* 3: 327-350.
- Kullberg M, Nilsson MA, Arnason U, Harley EH, et al. (2006). Housekeeping genes for phylogenetic analysis of eutherian relationships. *Mol. Biol. Evol.* 23: 1493-1503.
- Loss-Oliveira L, Aguiar BO and Schrago CG (2012). Testing synchrony in historical biogeography: the case of new world primates and hystricognathi rodents. *Evol. Bioinform. Online* 8: 127-137.
- Nei M and Glazko GV (2002). Estimation of divergence times for a few mammalian and several primate species. *J. Hered.* 93: 157-164.
- Opazo JC, Wildman DE, Pritchitko T, Johnson RM, et al. (2006). Phylogenetic relationships and divergence times among New World monkeys (Platyrrhini, Primates). *Mol. Phylogenet. Evol.* 40: 274-280.
- Perelman P, Johnson WE, Roos C, Seuanez HN, et al. (2011). A molecular phylogeny of living primates. *PLoS Genet.* 7: e1001342.
- Plummer M, Nicky B, Cowles K and Vines K (2006). CODA: Convergence diagnosis and output analysis for MCMC. *R News* 6: 7-11.
- Poux C and Douzery EJ (2004). Primate phylogeny, evolutionary rate variations, and divergence times: a contribution from the nuclear gene IRBP. *Am. J. Phys. Anthropol.* 124: 1-16.
- Poux C, Chevret P, Huchon D, de Jong WW, et al. (2006). Arrival and diversification of caviomorph rodents and platyrrhine primates in South America. *Syst. Biol.* 55: 228-244.
- Rannala B and Yang Z (2003). Bayes estimation of species divergence times and ancestral population sizes using DNA sequences from multiple loci. *Genetics* 164: 1645-1656.

- Ranwez V, Delsuc F, Ranwez S, Belkhir K, et al. (2007). OrthoMaM: a database of orthologous genomic markers for placental mammal phylogenetics. *BMC Evol. Biol.* 7: 241.
- Schrager CG (2007). On the time scale of New World primate diversification. *Am. J. Phys. Anthropol.* 132: 344-354.
- Schrager CG and Russo CA (2003). Timing the origin of New World monkeys. *Mol. Biol. Evol.* 20: 1620-1625.
- Steiper ME and Young NM (2006). Primate molecular divergence dates. *Mol. Phylogenet. Evol.* 41: 384-394.
- Steiper ME and Young NM (2009). Primates (Primates). In: *The Timetree of Life* (Hedges SB and Kumar S, eds.). Oxford University Press.
- Takai M and Anaya F (1996). New specimens of the oldest fossil platyrrhine, *Branisella boliviana*, from Salla, Bolivia. *Am. J. Phys. Anthropol.* 99: 301-317.
- Thorne JL and Kishino H (2002). Divergence time and evolutionary rate estimation with multilocus data. *Syst. Biol.* 51: 689-702.
- Thorne JL, Kishino H and Painter IS (1998). Estimating the rate of evolution of the rate of molecular evolution. *Mol. Biol. Evol.* 15: 1647-1657.
- Williams BA, Kay RF and Kirk EC (2010). New perspectives on anthropoid origins. *Proc. Natl. Acad. Sci. U. S. A.* 107: 4797-4804.
- Wilson DE and Reeder DM (2005). *Mammal Species of the World - A Taxonomic and Geographic Reference*. The Johns Hopkins University Press, Baltimore.
- Yang ZH (2006). *Computational Molecular Evolution*. Oxford University Press.
- Yang ZH (2007). PAML 4: Phylogenetic analysis by maximum likelihood. *Mol. Biol. Evol.* 24: 1586-1591.
- Yang Z and Yoder AD (2003). Comparison of likelihood and bayesian methods for estimating divergence times using multiple gene loci and calibration points, with application to a radiation of cute-looking mouse lemur species. *Syst. Biol.* 52: 705-716.
- Yoder AD and Yang Z (2004). Divergence dates for Malagasy lemurs estimated from multiple gene loci: geological and evolutionary context. *Mol. Ecol.* 13: 757-773.